Protein-ligand Dissociation Rate Constant From All-atom Simulation

Ekaterina Maximova,[*,†,‡] Eugene B. Postnikov,[*,¶] Anastasia I. Lavrova,[*,§,‖] Vladimir Farafonov,[*,⊥] and Dmitry Nerukh[*,#]

†*Department of Nanobiotechnology, Alferov University, Khlopina street, 8/3 A, 194021 Saint Petersburg, Russia*

‡*Center for Molecular and Cellular Bioengineering, Technische Universität Dresden, Helmholtzstr. 10, 01069 Dresden, Germany*

¶*Department of Theoretical Physics, Kursk State University, Radishcheva Street, 33, 305000 Kursk, Russia*

§*Saint-Petersburg State University, 7/9 Universitetskaya Emb., Saint Petersburg, Russia*

‖*Saint-Petersburg State Research Institute of Phthisiopulmonology, 2-4 Ligovskiy Avenue, Saint-Petersburg, Russia*

⊥*V. N. Karazin Kharkiv National University, 4 Svobody sq., Kharkiv, 61022, Ukraine*

#*Department of Mathematics, Aston University, Birmingham, B4 7ET, UK*

E-mail: ekaterina.maximova@mailbox.tu-dresden.de; postnikov@kursksu.ru; aurebours@googlemail.com; farafonov@karazin.ua; D.Nerukh@aston.ac.uk

Abstract

Dissociation of a ligand isoniazid from a protein catalase was investigated using all-atom Molecular Dynamics (MD) simulations. Random Acceleration MD (τ-RAMD) was used where a random artificial force applied to the ligand facilitates its dissociation. We have suggested a novel approach to extrapolate such obtained dissociation

times to the zero-force limit assuming never attempted before universal exponential dependence of the bond strength on the applied force, allowing direct comparison with experimentally measured values. We have found that our calculated dissociation time was equal to 36.1 seconds with statistically significant values distributed in the interval 0.2-72.0 s, that quantitatively matches the experimental value of 50 ± 8 seconds despite the extrapolation over nine orders of magnitude in time.

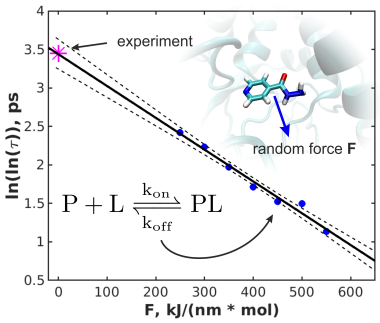

Figure 1: For Table Of Contents Only

Introduction The binding affinity of a compound, quantified by the dissociation constant K_D, is the key property of the compound's molecule for drug design. K_D is defined as the ratio of the rate constants for dissociation and association processes in the protein-ligand system, $K_D = \frac{k_{\text{off}}}{k_{\text{on}}}$, where $k_{\text{off(on)}}$ is the dissociation (association) rate constant and $\tau_{\text{off(on)}} = 1/k_{\text{off(on)}}$ is the dissociation (association) time.

Calculating on- and off-rates using molecular simulations is an active area of research, see[1–3] for recent reviews. Moreover, the kinetic properties, rather than K_D, are shown to correlate better with experimental drug efficacy[2–4].

All-atom Molecular Dynamics (MD) simulations can not in most cases calculate the kinetics of protein-ligand association and dissociation directly because experimental values are in the range of seconds, many orders of magnitude larger than currently accessible for straightforward MD. This is especially true for the dissociation time as it is much larger than the association time for drug candidates (which makes them good candidates). Therefore, a number of techniques for estimating the dissociation rates and elucidating the mechanisms of

dissociation using nano- and microsecond long MD simulations are employed[5]. Despite recent success, the calculated dissociation rates reproduce experimental values "within a factor of 2-20"[6], they are "still much smaller than the experimental value" (2 orders of magnitude)[7], or even they match the experimental values with "up to 4 orders of magnitude" error[8].

This discrepancy is emphasized recently[3] as one of the principal difficulties facing the MD approach to protein-ligand binding, highlighting that the primary factor affecting such large deviation is the "extrapolation by simulation methods for inferring long-timed event".

In this work, we use a method Random Acceleration MD (RAMD) in its variant called τ-RAMD[9,10] for obtaining dissociation times of a ligand isoniazid dissociating from a protein catalase. Isoniazid is the main drug for treating tuberculosis which targets catalase, a vital protein for functioning of *Mycobacterium tuberculosis*[11]. The method's idea consists of applying a small force to the ligand keeping the force constant in magnitude but changing periodically and randomly its direction in order to accelerate the unbinding. The simulation stops when the ligand reaches a predefined distance from the active site at which point it is considered dissociated and the time of dissociation is recorded. This approach is to certain extent similar to coupling spatial separation and chemical association/dissociation rate discussed in[12] but assures a simpler realisation required for the fully atomistic MD approach. As a result, τ-RAMD provides a set of dissociation times as a function of the magnitude of the applied force.

We here focus on the physical insight provided by such application of the random force to the system. Using recent results from the stochastic theory of reaction rates, we show that the simulated data can be used for estimating dissociation times that quantitatively match the experimental value of $\tau_{\text{off}}^{exp} = 50$ seconds.

Theory The computer experiment, realised through τ-RAMD, generates data in the form of the number of ligands that remain associated with protein at time t, $N(t)$. Normalised to 1 at zero time this gives the survival probability $\frac{N(t)}{N(0)}$ of finding the ligand associated with the protein at time t. Therefore, the first question for the theory is 'how

to define the dissociation time τ_{off} based on the survival probability $\frac{N(t)}{N(0)}$ for meaningful comparison with experimentally measured τ_{off}^{exp}'. As this value of τ_{off} obtained in simulation depends on the artificial applied force f, the second question is 'how to extrapolate the simulated dissociation times to zero force for comparison with real experiment'. As our data shows, answering both questions requires non-trivial physical approaches.

Definition of τ_{off} The origin of the stochastic theory of reaction rates including dissociation processes is dated back to the seminal work by H.A. Kramers[13] who considered the microscopic origin of macroscopic processes of chemical kinetics as random motion of thermally activated particles crossing a potential barrier. Further development of this theory can be found in comprehensive reviews[14–17].

In the simplest case of classical Kramers' kinetics, the probability density for spatiotemporal distribution of random particles satisfies the Fokker-Plank equation. Integrating its solution in the limits of the barrier gives the desirable time evolution of the survival probability $\frac{N(t)}{N(0)}$ relaxing as an exponential function; respectively, τ_{off} is defined as the inverse of the exponential coefficient.

However, there is also a possibility of the presence of anomalous kinetics that lead to the fractional Fokker-Plank equation with non-exponential relaxation behaviour[18]. It should be pointed out that such non-exponential, so-called "non-spectral", modes can exhibit themselves even in the case of the classical Fokker-Plank equation when initial conditions are taken from broad, highly non-stationary initial probability densities[19]. In this case a two-stage process of relaxation can be revealed when the leading power-law mode changes to the conventional spectral (exponential) relaxation mode during the time evolution of the system's dynamics[20].

Summarising, the dynamics of the ligand's probability to be dissociated from the protein can have two regimes:

(I) a non-exponential one at small times caused by non-equilibrium initial conditions originated from complex intermolecular interactions in the system under the influence of the

applied τ-RAMD external forces,

(II) a classical exponential relaxation at longer times when the above initial conditions are equilibrated.

The initial non-exponential regime is short-lived and, thus, undetectable by the experiment. We, therefore, assume that τ_{off} is defined by the second, much longer, regime and it is equal to the inverse of its exponential coefficient. In the following, for brevity, we use τ_{off} and τ as synonyms.

Dependence of dissociation time τ on the applied force Several works on lowering the potential barrier of dissociation under either the influence of additional applied forces or by velocity activating the particles within the context of dissociation or first passage time from a potential well exist[21–24]. However, these models are quite abstract and they deal with artificial numerical simulations, rather than with real biophysical systems.

To the best of our knowledge, the first attempt to take into account the influence of the external force f on the receptor-ligand coupling was proposed by G.I. Bell[25], who considered the characteristic lifetime of associated state τ in the simplest form

$$\tau = \nu_0 \exp\left[\left(E_0 - \gamma f\right)/k_B T\right], \tag{1}$$

where ν_0 is a function of natural frequency of oscillations of the system in the bound state that corresponds to the standard Kramers' theory. Respectively, when $f \to 0$, the value $\tau(f = 0)$ reduces to the inverse Kramers' dissociation constant for the unperturbed system. E_0 is the bond energy, γ is some phenomenological parameter, and k_B and T are Boltzmann's constant and the system's temperature.

Note that Eq. (1) can be formally considered as a solution of the ordinary differential equation

$$\frac{d\tau}{df} = -\frac{\gamma}{k_B T}\tau. \tag{2}$$

From the simplest point of view of dimensional analysis, the parameter γ has a meaning

of some characteristic length, which a particle should overcome under forcing which can be considered as work diminishing the initial free energy of the barrier/bond. Clearly, this work and, thus, γ depend on the force f. We here suggest a model by assuming that this characteristic "length" decreases with force in the same Boltzmann-like manner:

$$\gamma = \gamma_0 \exp\left[\left(-\gamma' f\right)/k_B T\right]. \tag{3}$$

A similar line of reasoning was used to describe the so-called "catch bonds" that increase their strength with growing applied force[26,27]. Thus, we hypothise that this behaviour has a universal character for complex biological molecules.

Substituting Eq. (3) into Eq. (2), we obtain the differential equation

$$\frac{d\tau}{df} = -\frac{\gamma_0}{k_B T} e^{-\frac{\gamma' f}{k_B T}} \tau, \tag{4}$$

which can be easily solved by the method of separation of variables:

$$\tau = \tau_0 e^{\frac{\gamma_0}{\gamma'}\left(e^{-\frac{\gamma' f}{k_B T}} - 1\right)}, \tag{5}$$

where $\tau_0 = \nu_0 \exp\left[-E_0/k_B T\right]$ is the dissociation time for the unperturbed system. It is easy to see that τ_0 is equal to the solution (5) with $f = 0$. Towards the large forces, the solution (5) tends asymptotically to $\tau_\infty = \tau_0 \exp\left(-\gamma_0/\gamma'\right)$. It has a finite value that is agreed with the stochastic character of the model since even if the applied force destroys the barrier completely, a particle needs some time to leave the vicinity of its initial position via a random walk. At the same time, $\tau_\infty << \tau_0$ in multiple orders of magnitude, i.e. $\gamma' << \gamma_0$. Note also that for weak perturbation forces, $\gamma' f/k_B T << 1$, the solution (5) reduces to the Bell's expression (1) with $\gamma = \gamma_0$.

Eq. (5) can be linearised as

$$\ln\left(\ln\left(\frac{\tau}{\tau_0}e^{\frac{\gamma_0}{\gamma'}}\right)\right) = \ln\left(\frac{\gamma_0}{\gamma'}\right) - \frac{\gamma'}{kT}f. \tag{6}$$

This expression contains true dimensionless and strictly positive arguments of logarithms but they contain unknown parameters not accessible in direct measurements or simulations. Whence, Eq. (6) plays a role of a qualitative argument, which demonstrates a possible origin of the functional dependence in the form of doubly logarithmic dependence of the escape time on the applied force. Since Eq. (6) contains a combination of phenomenological parameters, it is more convenient to apply some rescaling intended to get a simpler expression for the further analysis of simulated data.

Rescaling the escape time τ by the constant $\frac{e^{\gamma_0/\gamma'}}{\tau_0}$, $\tilde{\tau} = \tau\frac{e^{\gamma_0/\gamma'}}{\tau_0}$ we obtain $\tilde{\tau}_0 = \tau_0\frac{e^{\gamma_0/\gamma'}}{\tau_0} = e^{\gamma_0/\gamma'}$ from which $\gamma_0/\gamma' = \ln(\tilde{\tau}_0)$, $\ln\left(\frac{\gamma_0}{\gamma'}\right) = \ln\left(\ln\left(\tilde{\tau}_0\right)\right)$ and Eq. (6) becomes

$$\ln\left(\ln\left(\tilde{\tau}\right)\right) = \ln\left(\ln\left(\tilde{\tau}_0\right)\right) - \frac{\gamma'}{kT}f, \tag{7}$$

providing a linear dependence between the double logarithm of the rescaled dissociation time and the applied force. Clearly, for $f = 0$ the dissociation time τ is equal to τ_0 for non-scaled dissociation times.

Molecular model and simulation details Catalase from *Mycobacterium tuberculosis* (*Mt*KatG) is the target for isoniazid. However, no experimental atomistic data is available for setting the initial structure of the complex for MD. Fortunately, *Mycobacterium tuberculosis* catalase (*Mt*KatG) and *Burkholderia pseudomallei* catalase (*Bp*KatG) have very similar atomic structures and activity against isoniazid[28]. As no experimental structure of isoniazid-bound *Mt*KatG is available in the Protein Data Bank[29], atomic coordinates were obtained by superimposing the crystal structures of *Mt*KatG (PDB: 1sj2) and the complex *Bp*KatG-INH (PDB: 5syi) using UCSF Chimera[30]. Molecular Dynamics simulation details are provided in Supporting Information.

Multiple τRAMD calculations were carried out by applying different forces to the ligand: 550, 500, 450, 400, 350, 300 and 250 $\frac{\text{kJ}}{\text{mol}\cdot\text{nm}}$. If the distance between the centers of mass of the ligand and the protein changed by less than 0.025 nm, the direction of the force was randomly altered. The maximum COMs distance at which the ligand was guaranteed to leave the protein surface was set to 5 nm. At each force value, a number of runs, $N(0)$ (up to 200), was performed using identical initial coordinates and velocities with the only different parameter being the random seed for random force generation. Since isoniazid is a small ligand and its conformation and position in the active site hardly change over time, sampling of the bound state (i.e. obtaining several starting structures) was not necessary and did not affect the final result (the dissociation time).

Data processing For each force value, the set of dissociation times was recalculated to the dependency of the survival probability on the simulation time. For a time moment t the count $N(t)$ was calculated as a total number of complexes that have not dissociated at this time. It equals to the number of τ-RAMD runs in the set (for the given value of f) having duration longer than t. To obtain survival probability, $N(t)$ was then divided by the total number of runs $N(0)$ in the set, t ranged from zero to the duration of the longest run in the set, and $N(t)/N(0)$ changed from unity at $t = 0$ to zero at the last t value, Fig. 2.

Obtaining dissociation times Clearly, the survival probability data points $N(t)/N(0)$ for each force demonstrate two regimes, Fig. 2. During the first stage, the decay follows a bell-shaped curve, which can be accurately fitted as $\ln\left[-\ln(N(t)/N(0))\right] = p\ln(t) + p\ln(t_0)$, where p is the power index and t_0 is some characteristic time that results in the revealed time dependence $N(t) = N_0\exp(-(t/t_0)^p)$ shown as the black dashed curve in Fig. 2. For these two examples p are equal to 1.4 and 1.6.

However, after some time τ_{frac} the survival probability exhibits drastic change in the dynamics starting to follow a linear dependence of $\ln(N(t)/N_0)$ vs. t that corresponds to the usual relaxation process $\frac{dN(t)}{dt} = -\lambda N(t)$ with the decay rate λ determining the dissociation time τ. By the end of the exponential decay, the remained long-lasting complexes form

"shelves" with constant N values, which distort the slope of the fitted line. These "shelves" were formed by a very small number of non-dissociating complexes with step-wise changes that are far from the continuous dependence of the model for fitting the data. To define the threshold of statistically significant data and to obtain reliable fit, the values at the end were cut off one by one until the slope stops changing (see Fig. S1 in Supporting Information for a representative example). In some cases (as in Fig. 2 (a)) all the values were retained for fitting as cutting off the end points did not change the slope.

The dissociation times reciprocal to the rate, $\tau = \frac{1}{\lambda}$, for all forces are listed in Table 1 as well as the times of the crossover between the two regimes. Note that the values of τ and τ_{frac} are close to each other that supports the interpretation of the initial regime as significantly non-equilibrium transient processes taking place at times shorter than the characteristic relaxation time of the system. Thus, it was excluded from the further analysis. The fitted curves for all values of the force f are included in Supporting Information.

Extrapolation to zero force The dependence of the obtained values of the dissociation time τ on the applied force f per mole was reduced to the linearised form by sequential twice logarithmic transformation as shown in Fig. 3. The apparent linearity in the dependence on f confirms the theoretical model (7). The linear fit of these values

$$\ln\left(\ln(\tilde{\tau})\right) = \ln\left(\ln(\tilde{\tau}_0)\right) - \kappa f \tag{8}$$

was carried out using the standard Curve Fitting Toolbox of MATLAB, which uses the QR factorization algorithm. Note that we used dimensional times (ps) obtained from the data processing procedure for the fitting to avoid unnecessary complications with multiple parameters introduced when we considered a possible theoretical model, which leads to such double logarithmic functional form. Since we are interested in the value of τ_0 only, this kind of fitting directly gives the desired parameter as the original τ_0 coincides with the scaled $\tilde{\tau}_0$.

Results and Discussion Fitting data from Table 1 using Eq. (8) results in $R^2 = 0.978$

and $RMSE = 0.073$ for the chosen scaled units.

This procedure of fitting gives the average value of the slope equal to $\kappa = 0.0041$ with the confidence intervals from 0.0038 to 0.0044 at the level of standard deviation. The second fitting parameter of the fitted straight line (8) has the average value $\ln(\ln(\tau_0)) = 3.441$ with the confidence interval from 3.315 to 3.563 at the level of standard deviation. The numerical values correspond to picoseconds as the dimensionality of time.

The calculated $\ln(\ln(\tau_0))$ assumes normal distribution around the found average value. However, exponentiating it twice to obtain τ_0 significantly changes the type of the probability distribution and requires more sophisticated procedure for determining τ_0 and its uncertainty. We evaluated them using the NIST Uncertainty Machine[31] with Monte-Carlo algorithm simulating an ensemble of 10^6 realisations. After the transformation the probability distribution becomes highly long-tailed and skewed with a power law tail, which can lead to divergent statistical moments (see Fig. S3 in Supporting Information for the distribution plots).

For this type of distributions the robust statistical measure of the most probable value is the median, which in our case was equal to $M(\tau_0) = 36.1$ seconds. Statistically significant deviations from this value are quantified by the median of the absolute value of the deviations $M(|\tau_0 - M(\tau_0)|)$, equal to 35.9 seconds in our case and making the statistically significant values distributed between 36.1-35.9=0.2 and 36.1+35.9=72.0 seconds.

Summarising, the found extrapolated value of τ_0 is 36.1 seconds, with statistically significant boundaries 0.2 and 72.0 s, that matches the experiential value of 50 ± 8 s quantitatively within the uncertainties of extrapolation and experiment.

Conclusions In conclusion, we have applied the τ-RAMD methodology to obtain the probabilities of the ligand to dissociate from the protein. We have also suggested a theory for these probabilities that describes their time evolution according to two regimes, a non-exponential for small times and standard exponential for longer times. We have identified these two regimes in the data generated by the simulations. Finally, we suggested

Table 1: Dissociation times τ and moments of crossover from fractional exponential to classical relaxation regime τ_{frac}

f, kJ/(nm · mol)	τ, ps	τ_{frac}, ps
250	78397	70000
300	11044	10000
350	1319	1300
400	259	300
450	98	106
500	87	150
550	22	24

a model that allows to extrapolate the obtained dissociation times to the zero-force value that quantitatively match the experimentally measured value of 50 seconds. This is in contrast to the original τ-RAMD approach where no such extrapolation was attempted. Importantly, the extrapolation has been done through nine orders of magnitude in the value of τ, from nanoseconds to seconds. Nevertheless, the extrapolated value quantitatively reproduces the experiential one, in contrast to the majority of current methods described in literature.

Our model can be used in other settings, for example in immunology for an alternative calculation of the "dissociation time" as a relation of the "immunological synapse" time[32–34].

Acknowledgments We acknowledge the use of Athena at HPC Midlands+, which was funded by the EPSRC on grant EP/P020232/1, in this research, as part of the HPC Midlands+ consortium. V.F. expresses his gratitude to the Ministry of Education and Science of Ukraine for financial support in the project "Molecular docking for express identification of new potential drugs" (0119U002550). The collaboration was supported by the program H2020-MSCA-RISE-2018, project AMR-TB, grant ID: 823922.

Supporting Information Available Molecular Dynamics simulation details, example of the "shelves" influence on the slope of the exponential regime (Fig. S1), survival probabilities for all values of the force fitted with 2 regimes (Fig. S2), Monte-Carlo simulated distributions of the fitted parameter $\ln(\ln(\tau_0))$ and transformed τ_0 (Fig. S3).

References

(1) Decherchi, S.; Cavalli, A. Thermodynamics and Kinetics of Drug-Target Binding by Molecular Simulation. *Chem. Rev.* **2020**, *120*, 12788–12833.

(2) Nunes-Alves, A.; Kokh, D. B.; Wade, R. C. Recent progress in molecular simulation methods for drug binding kinetics. *Curr. Opin. Struct. Biol.* **2020**, *64*, 126–133.

(3) Ahalawat, N.; Mondal, J. An appraisal of computer simulation approaches in elucidating biomolecular recognition pathways. *J. Phys. Chem. Lett.* **2021**, *12*, 633–641.

(4) Bruce, N. J.; Ganotra, G. K.; Kokh, D. B.; Sadiq, S. K.; Wade, R. C. New approaches for computing ligand–receptor binding kinetics. *Curr. Opin. Struct. Biol.* **2018**, *49*, 1–10.

(5) Mapplebeck, S.; Booth, J.; Shalashilin, D. Simulation of protein pulling dynamics on second time scale with boxed molecular dynamics. *J. Chem. Phys.* **2021**, *155*, 085101.

(6) Wolf, S.; Lickert, B.; Bray, S.; Stock, G. Multisecond ligand dissociation dynamics from atomistic simulations. *Nat. Commun.* **2020**, *11*.

(7) Capelli, R.; Lyu, W.; Bolnykh, V.; Meloni, S.; Olsen, J. M. H.; Rothlisberger, U.; Parrinello, M.; Carloni, P. Accuracy of molecular simulation-based predictions of k_off values: a metadynamics study. *J. Phys. Chem. Lett.* **2020**, *11*, 6373–6381.

(8) Ribeiro, J. M. L.; Tsai, S.-T.; Pramanik, D.; Wang, Y.; Tiwary, P. Kinetics of Ligand–Protein Dissociation from All-Atom Simulations: Are We There Yet? *Biochemistry* **2018**, *58*, 156–165.

(9) Kokh, D. B.; Doser, B.; Richter, S.; Ormersbach, F.; Cheng, X.; Wade, R. C. A workflow for exploring ligand dissociation from a macromolecule: Efficient random acceleration molecular dynamics simulation and interaction fingerprint analysis of ligand trajectories. *J. Chem. Phys.* **2020**, *153*, 125102.

(10) Kokh, D. B.; Amaral, M.; Bomke, J.; Grädler, U.; Musil, D.; Buchstaller, H.-P.; Dreyer, M. K.; Frech, M.; Lowinski, M.; Vallee, F.; Bianciotto, M.; Rak, A.; Wade, R. C. Estimation of Drug-Target Residence Times by τ-Random Acceleration Molecular Dynamics Simulations. *J. Chem. Theory Comput.* **2018**, *14*, 3859–3869.

(11) Unissa, A. N.; Subbian, S.; Hanna, L. E.; Selvakumar, N. Overview on mechanisms of isoniazid action and resistance in Mycobacterium tuberculosis. *Infect. Genet. Evol.* **2016**, *45*, 474–492.

(12) Jagger, B. R.; Lee, C. T.; Amaro, R. E. Quantitative ranking of ligand binding kinetics with a multiscale milestoning simulation approach. *J. Phys. Chem. Lett.* **2018**, *9*, 4941–4948.

(13) Kramers, H. A. Brownian motion in a field of force and the diffusion model of chemical reactions. *Physica* **1940**, *7*, 284–304.

(14) Hänggi, P.; Talkner, P.; Borkovec, M. Reaction-rate theory: fifty years after Kramers. *Rev. Mod. Phys.* **1990**, *62*, 251.

(15) Ebeling, W.; Schimansky-Geier, L.; Romanovsky, Y. M. *Stochastic dynamics of reacting biomolecules*; World Scientific (Singapore), 2002.

(16) Pollak, E.; Talkner, P. Reaction rate theory: What it was, where is it today, and where is it going? *Chaos* **2005**, *15*, 026116.

(17) Bernetti, M.; Masetti, M.; Rocchia, W.; Cavalli, A. Kinetics of drug binding and residence time. *Ann. Phys. Chem.* **2019**, *70*, 143–171.

(18) Dybiec, B.; Sokolov, I. M. Estimation of the smallest eigenvalue in fractional escape problems: Semi-analytics and fits. *Comput. Phys. Commun.* **2015**, *187*, 29–37.

(19) Toenjes, R.; Sokolov, I. M.; Postnikov, E. B. Nonspectral Relaxation in One Dimensional Ornstein-Uhlenbeck Processes. *Phys. Rev. Lett.* **2013**, *110*, 150602.

(20) Thiel, F.; Sokolov, I. M.; Postnikov, E. B. Nonspectral modes and how to find them in the Ornstein-Uhlenbeck process with whiteμ-stable noise. *Phys. Rev. E* **2016**, *93*, 052104.

(21) Lin, H.-J.; Chen, H.-Y.; Sheng, Y.-J.; Tsao, H.-K. Bell's expression and the generalized Garg form for forced dissociation of a biomolecular complex. *Phys. Rev. Lett.* **2007**, *98*, 088304.

(22) Friddle, R. W. Unified model of dynamic forced barrier crossing in single molecules. *Phys. Rev. Lett.* **2008**, *100*, 138302.

(23) Abkenar, M.; Gray, T. H.; Zaccone, A. Dissociation rates from single-molecule pulling experiments under large thermal fluctuations or large applied force. *Phys. Rev. E* **2017**, *95*, 042413.

(24) Scacchi, A.; Brader, J. M.; Sharma, A. Escape rate of transiently active brownian particle in one dimension. *Phys. Rev. E* **2019**, *100*, 012601.

(25) Bell, G. I. Models for the specific adhesion of cells to cells. *Science* **1978**, *200*, 618–627.

(26) Pereverzev, Y. V.; Prezhdo, O. V. Force-induced deformations and stability of biological bonds. *Phys. Rev. E* **2006**, *73*, 050902.

(27) Prezhdo, O. V.; Pereverzev, Y. V. Theoretical aspects of the biological catch bond. *Acc. Chem. Res.* **2009**, *42*, 693–703.

(28) Singh, R.; Wiseman, B.; Deemagarn, T.; Jha, V.; Switala, J.; Loewen, P. C. Comparative study of catalase-peroxidases (KatGs). *Arch. Biochem. Biophys.* **2008**, *471*, 207–214.

(29) Protein Data Bank: the single global archive for 3D macromolecular structure data. *Nucleic Acids Res.* **2019**, *47*, D520–D528.

(30) Pettersen, E. F.; Goddard, T. D.; Huang, C. C.; Couch, G. S.; Greenblatt, D. M.; Meng, E. C.; Ferrin, T. E. UCSF Chimera—a visualization system for exploratory research and analysis. *J. Comput. Chem.* **2004**, *25*, 1605–1612.

(31) Lafarge, T.; Possolo, A. The NIST uncertainty machine. *NCSLI Measure* **2015**, *10*, 20–27.

(32) Chattopadhyay, A. K.; Burroughs, N. J. Close contact fluctuations: The seeding of signalling domains in the immunological synapse. *Europhys. Lett.* **2007**, *77*, 48003.

(33) Bush, D. R.; Chattopadhyay, A. K. Contact time periods in immunological synapse. *Phys. Rev. E* **2014**, *90*, 042706.

(34) Bush, D. R.; Chattopadhyay, A. K. Temporal dynamics in an immunological synapse: Role of thermal fluctuations in signaling. *Phys. Rev. E* **2015**, *92*, 012706.

(a) $F = 350$ kJ/(nm · mol)

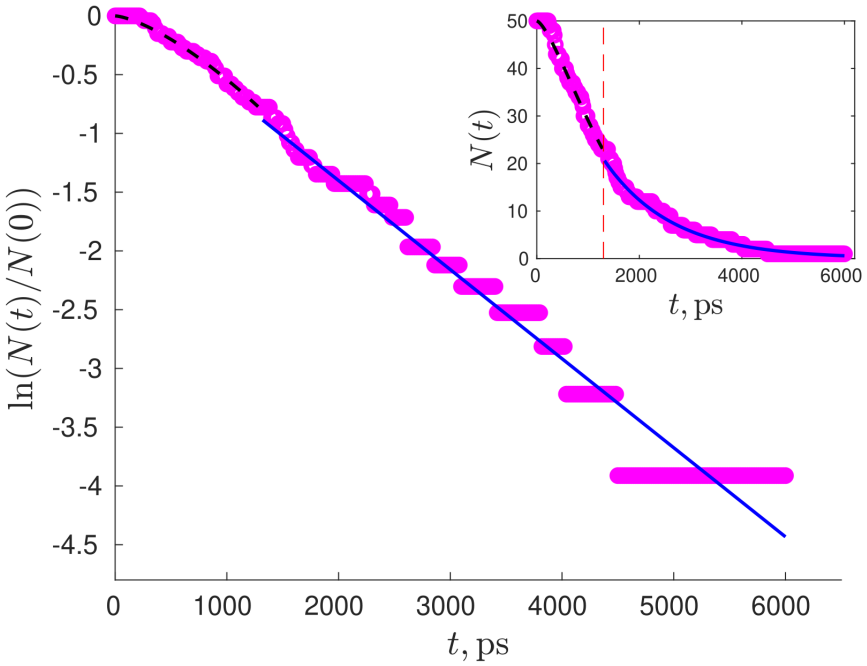

(b) $F = 500$ kJ/(nm · mol)

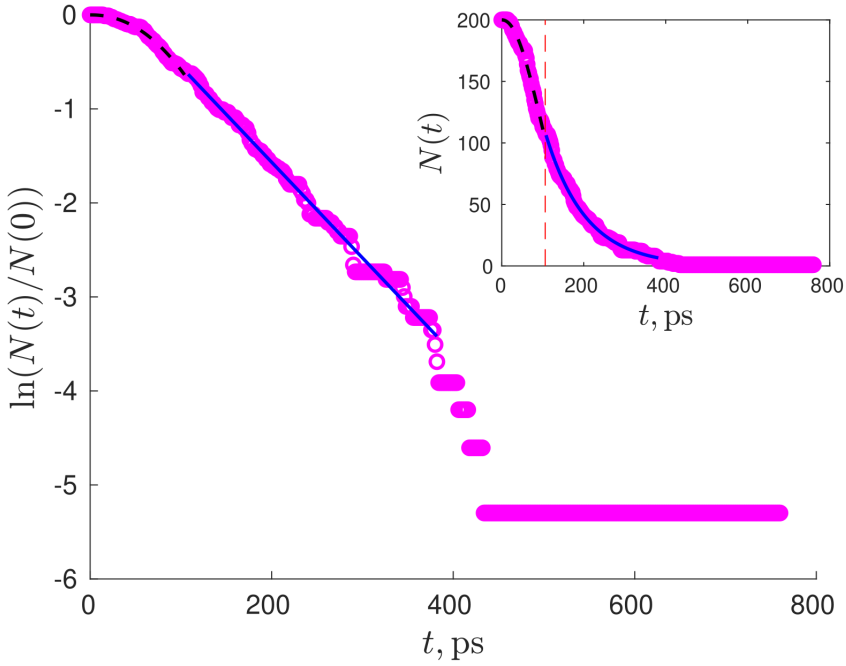

Figure 2: Fitting the probability of the ligand to remain associated with the protein using models for two regimes (see text); the results for the external force strength equal to 350 kJ/(nm · mol) (a) and 500 kJ/(nm · mol) (b) are shown; black dashed line – non-exponential model, blue line – exponential model, red dash-dot line – the moment of switching between the models; the fitted values of the parameters are in Table 1.

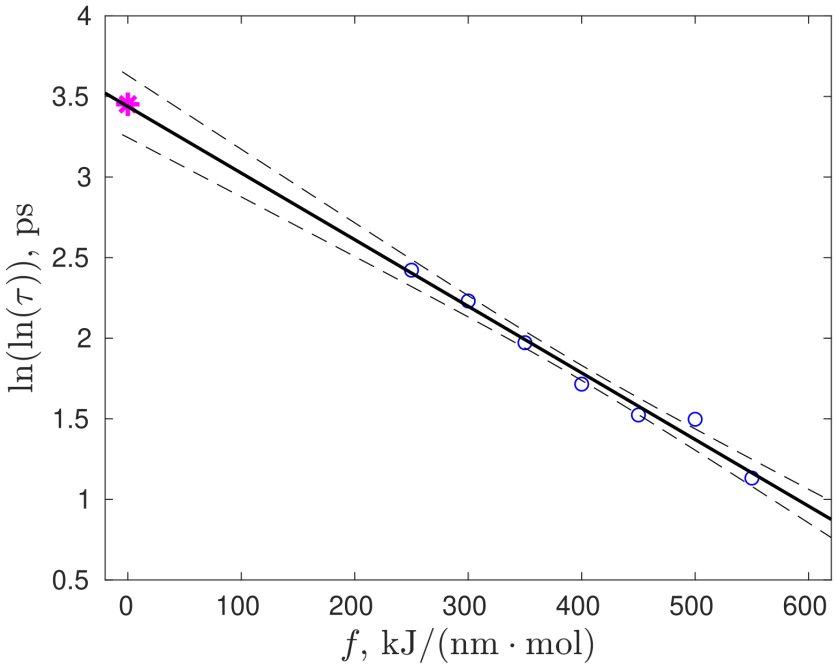

Figure 3: The sequence of dissociation times determined from MD simulations linearised by a coordinate transformation as a function of the applied forces per mole (circles) and their linear fitting (solid line). The dashed curves denote the prediction bounds with a confidence level equal to the standard deviation. The asterisk marks the experimental value.